

Performance uniformity analysis of a wire-grid polarizer in imaging polarimetry

Donghyun Kim

The polarimetric performance nonuniformity of a wire-grid polarizer (WGP) used in imaging polarimetry is investigated with a simple numerical model. The simulation results based on rigorous coupled-wave analysis show that the aperture ratio between the entrance pupil and the WGP significantly affects the uniformity among pixels of a WGP. Even with a WGP smaller than an imaging aperture, the results suggest that the design avoids incurring a Rayleigh anomaly, which causes a substantial increase in polarimetric nonuniformity. Minimizing the variation due to the characteristics of a WGP is important to reduce the likelihood of an error in imaging polarimetry. © 2005 Optical Society of America

OCIS codes: 050.1950, 120.5410, 230.5440, 260.5430.

1. Introduction

A wire-grid polarizer (WGP) is extensively used as a polarization-sensitive element in various applications, ranging from remote sensing to displays to biomedical engineering, because of the excellent polarization performance and planar structure that allow it to be easily pixilated and integrated into other optoelectronic devices.^{1–5} The wire grids of a WGP are made of a good conductor; if the electric field is parallel to the wire grids (TE polarization), they absorb and do not sustain an electric vector in the surface. This makes the field strength of a TE polarization order propagating parallel to the surface much smaller than that of a TM order whose electric field is orthogonal to the wires of a WGP. In other words, an electric field oscillates orthogonally for the most part with respect to grating wires as the light is transmitted through a wire-grid grating polarizer.

This study theoretically investigates the performance uniformity in a standard implementation of imaging polarimetry that is based on a WGP and its implications in the design of such a system. A WGP shows good optical stability with respect to variation of the polar angle and azimuthal rotation.^{6,7} However, overall uniformity of polarization discrimina-

tion across a WGP and its effect on the performance of an imaging polarimetric system with a WGP have not been fully explored previously.^{4,8–11}

A simplified optical setup of imaging polarimetry that does not employ any stop is described in Fig. 1, where objects at a distance are imaged by a lens (L) onto a pixilated forward-looking WGP. Since an off-axis pixel captures an object at an angle that varies from pixel to pixel over a WGP, each pixel shows different polarization characteristics. The variation of polarization characteristics across WGP pixels indicates that an identical object is measured with unidentical intensity data by different WGP pixels, depending to a large extent on the line of sight of an object relative to the optical axis of the imaging polarimetry system. The pixel-to-pixel variation of the polarimetric detection of a WGP can potentially lead to misjudgment and should be minimized. In particular, many imaging polarimeters intend to obtain the Stokes parameters (S_0, S_1, S_2, S_3) of an incident scene based on intensity measurement data such that¹²

$$\begin{aligned} S_0 &= I(\alpha = 0^\circ, \varepsilon = 0) + I(\alpha = 90^\circ, \varepsilon = 0), \\ S_1 &= I(\alpha = 0^\circ, \varepsilon = 0) - I(\alpha = 90^\circ, \varepsilon = 0), \\ S_2 &= I(\alpha = 45^\circ, \varepsilon = 0) - I(\alpha = 135^\circ, \varepsilon = 0), \\ S_3 &= I(\alpha = 45^\circ, \varepsilon = \pi/2) - I(\alpha = 135^\circ, \varepsilon = \pi/2), \end{aligned} \quad (1)$$

where α is the orientation of a WGP pixel with respect to the reference axis and ε is a retardation between electric field components. It is apparent that the non-uniform polarimetric discrimination of WGP pixels causes the Stokes parameters of an identical object to be measured differently. For an implementation

D. Kim (kimd@yonsei.ac.kr) is with the School of Electrical and Electronic Engineering, Yonsei University, Seoul, South Korea 120-749.

Received 25 February 2005; revised manuscript received 21 April 2005; accepted 29 April 2005.

0003-6935/05/265398-05\$15.00/0

© 2005 Optical Society of America

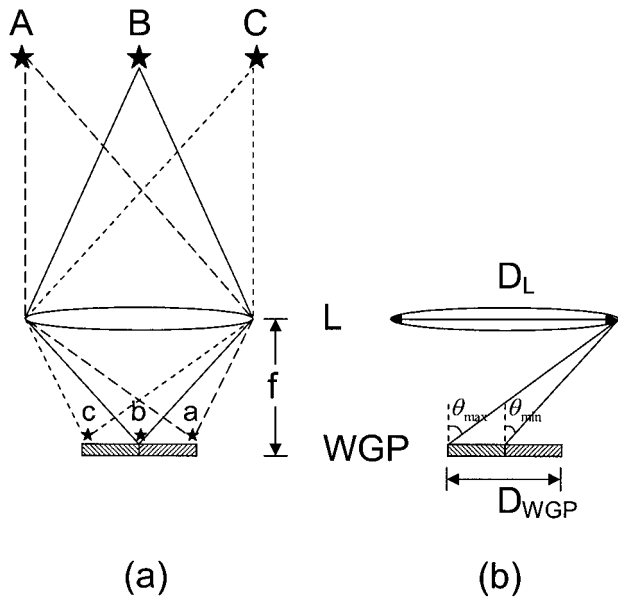


Fig. 1. (a) Simplified configuration of imaging polarimetry with a WGP. An object (A, B, or C) is imaged by a lens (L) in the image plane (a, b, or c) formed on a WGP. Objects are assumed to be at an infinite distance. (b) θ_{\max} and θ_{\min} used in Eqs. (2)–(4). D_L and D_{WGP} are the diameter of the lens and the WGP, respectively. f is the focal length of the imaging lens.

based on a rotating polarizer this variation may be compensated by calculating a Mueller matrix, which is a transfer function between input and output Stokes parameters. However, the compensation cannot be complete for a WGP pixel that integrates subpixels of different orientations because the non-uniformity also varies with subpixels. The goal of this study, therefore, is to understand the effect of various design parameters on the variation and uniformity of the polarimetric performance when imaging polarimetry employs a WGP as a polarization-sensitive element and furthermore to contrive an implementation that minimizes the variation.

This paper is organized as follows: A numerical model is described in Section 2, and the results are presented in Section 3. Implications of the presented results to the design of an imaging polarimetry implementation are discussed in Section 4, which is followed by concluding remarks in Section 5.

2. Numerical Model

A WGP for a midwave infrared (MWIR) wave band of $3 < \lambda < 5 \mu\text{m}$ is introduced. Although wire grids of different orientations are typically pixilated in a polarization sensor to obtain the full Stokes parameters of an incident scene by detecting multiple polarization components simultaneously,^{9,13,14} the model setup shown in Fig. 1 of a pixilated WGP assumes the pixels of the wire grids are in an identical direction for simplicity. In particular, in the next section, a WGP with wires of different orientations will be briefly discussed. In Fig. 1, an object is imaged by an imaging lens with an f -number of $f/\# = 2$ in the image plane on a sensor that is assumed to be in contact

with a WGP. D_L and D_{WGP} denote the diameter of the imaging lens and the WGP, respectively. f is the focal length of lens L. As a measure of the polarization contrast of a polarizer, an extinction ratio (ER), defined as the intensity ratio between TM and TE polarization components transmitted through a WGP, is introduced. The transmittance of the TM polarization component is also important, since poor TM transmittance requires a highly sensitive sensor element even with an excellent ER. For the numerical simulation, well-established rigorous coupled-wave analysis, also known as the Fourier modal method, was used in this study.¹⁵

As for a pixel of a WGP, a simple grating structure is considered, in which a grating of gold is modeled on top of a silicon substrate. The grating has a square profile and a 50% fill factor. Typical semiconductor fabrication processes stipulate that a grating cannot be made too thick once a grating period is given. Also, the grating thickness should be large enough not to create evanescent modes at the top and bottom grating interfaces that may tunnel through the grating and participate in the multiple beam interference. The grating depth d is fixed at 250 nm in this study, unless otherwise noted. Optical parameters for gold and silicon were obtained from Ref. 16 and interpolated for the MWIR.

3. Results

The performance uniformity of a WGP correlates with the ER and the transmittance of the TM polarization at a maximum incidence angle that the farthest off-axis pixel captures in an input scene ($\theta_{\text{in}} = \theta_{\max}$), normalized to that of an on-axis pixel ($\theta_{\text{in}} = \theta_{\min}$). The normalized ER (NER) and normalized TM transmittance (NTMT) are defined as

$$\text{NER} = \frac{\text{ER}(\theta_{\text{in}} = \theta_{\max})}{\text{ER}(\theta_{\text{in}} = \theta_{\min})}, \quad \text{NTMT} = \frac{T(\theta_{\text{in}} = \theta_{\max})}{T(\theta_{\text{in}} = \theta_{\min})}, \quad (2)$$

where T in Eq. (1) denotes transmittance. From Fig. 1, it can be easily shown that

$$\begin{aligned} \tan \theta_{\max} &= \frac{D_L + D_{\text{WGP}}}{2f} \\ &= \frac{D_L}{2f} \left(1 + \frac{D_{\text{WGP}}}{D_L} \right) \\ &= \frac{1}{2f/\#} \left(1 + \frac{D_{\text{WGP}}}{D_L} \right), \end{aligned} \quad (3)$$

$$\tan \theta_{\min} = \frac{D_L}{2f} = \frac{1}{2f/\#}. \quad (4)$$

The NER and NTMT characterize the maximum variation of an ER and TM transmittance with which different pixels of a WGP measure an identical object and thus can serve as a metric to quantify the polarimetric performance uniformity of a given WGP. The ratio of the ER and TM transmittance at $\theta_{\text{in}} = \theta_{\max}$ to

that of $\theta_{in} = 0^\circ$ was also investigated as a performance measure that considers that the light incident on a pixel takes a range of incidence angles including normal incidence. The analysis showed the same trends with larger variations compared with the results based on the NER and NTMT defined in Eq. (2).

As the NER and NTMT deviate further from unity, either higher or lower, the WGP performance is less uniform. For example, if $NER = 1.2$ and $NTMT = 1.0$ for a WGP, it indicates that the WGP shows 20% nonuniformity in the ER while the detected TM transmittance is fairly uniform. Equations (3) and (4) imply that a higher $f/\#$ of an imaging lens or a smaller WGP leads to lower θ_{max} and a NER and NTMT closer to unity, which indicates improved performance uniformity.

Figure 2 presents the NER and NTMT with an

aperture ratio (D_{WGP}/D_L) for various grating periods (Λ) at $\lambda = 3 \mu\text{m}$ while the f -number of the lens is fixed at $f/\# = 2$. Note that only the zeroth diffraction order was considered in calculating the NER and NTMT and edge effects for outermost pixels were neglected. Figure 2 shows a general tendency that the NER and NTMT grow larger with a higher D_{WGP}/D_L , although the specific nature depends on the grating period. For small grating periods, the NER and NTMT grow monotonically. On the other hand, for larger grating periods, higher-order diffraction is excited at a large incidence angle due to a Rayleigh anomaly, affecting the ratios significantly. Generally, a Rayleigh anomaly, which is due to energy redistribution in the creation or cutoff of a higher diffraction order, affects the performance of a WGP adversely, since an ER and TM transmittance can be considerably low near a Rayleigh anomaly and the presence of higher diffraction orders can produce additional noise in the polarimetric sensor system. From the grating equation describing the momentum-matching condition between multiple diffraction orders, combined with Snell's law, the Rayleigh anomaly occurs if

$$\sin \theta_{in} = n_s \left(1 - \frac{m\lambda}{n_s \Lambda} \right), \quad (5)$$

where n_s is the refractive index of a silicon substrate and m is an integer that represents a diffraction order. Equation (5) gives the aperture ratio at a Rayleigh anomaly as 1.77 for $\Lambda = 0.75 \mu\text{m}$ and 0.91 for $\Lambda = 1 \mu\text{m}$, which confirms that the anomalous features shown in Fig. 2 are associated with a Rayleigh anomaly. The deviation in the ER and the TM transmittance are substantial even if a WGP is designed with fine wire grids. At $D_{WGP}/D_L = 1.0$ and $\Lambda = 0.5 \mu\text{m}$, the deviation of the ER across pixels of a WGP is approximately 13%, whereas that of the TM transmittance is less than 5%. In Fig. 2, it is interesting to see higher performance for off-axis pixels with a larger ER and TM transmittance, whereas pixels near the optical axis show worse performance when a Rayleigh anomaly does not occur.

Figure 3 compares the effect of the grating depth d of wire grids on the NER. Although thicker wire grids provide a much higher ER and TM transmittance in general, Fig. 3 shows that there is no clear benefit to thicker wire grids in terms of the performance uniformity since the improvement is negligible for up to a moderate aperture ratio and is only visible for a WGP with a large grating period and D_{WGP}/D_L .

In practice, a WGP is limited in size and expensive to enlarge. Also, if $D_{WGP}/D_L > 1$, pixels located on the edge of the WGP are subject to vignetting even for an on-axis object. Therefore, a WGP is typically smaller than an imaging aperture. With $D_{WGP}/D_L = 1.0$ as a worst-case scenario, Fig. 4 shows the NER and NTMT with grating periods. It is noted that the deviation of an ER is always lower than that of transmittances. An obviously significant effect of a Rayleigh anomaly in the range of $\Lambda = 0.8\text{--}1.0 \mu\text{m}$

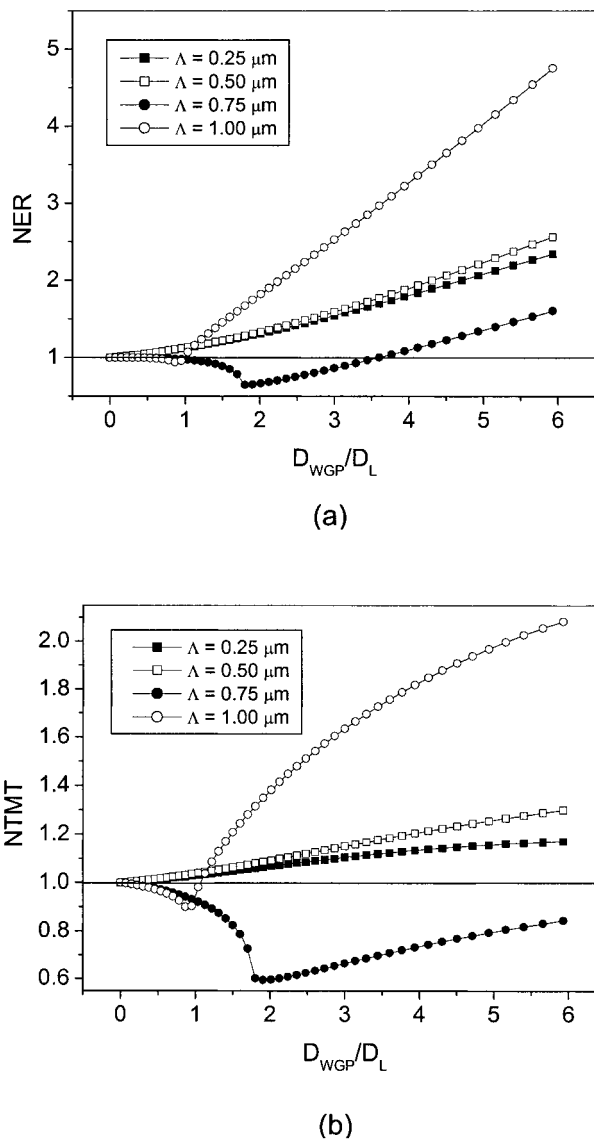


Fig. 2. (a) NER and (b) NTMT defined in Eq. (1) with D_{WGP}/D_L as the grating period varies at $\lambda = 3 \mu\text{m}$. The f -number of an imaging lens is assumed to be fixed at 2. A solid line denoting $NER = 1$ and $NTMT = 1$ is also shown as a reference.

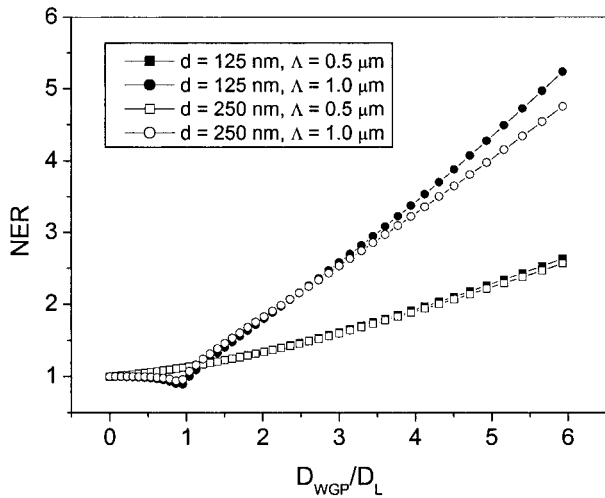


Fig. 3. Effect of the grating depth of wire grids on the uniformity.

indicates that the Rayleigh anomaly not only degrades ERs and the transmittance of a WGP, but it also substantially deteriorates the uniformity. Figure 5, on the other hand, presents the uniformity variation for $\Lambda = 0.5$ and $1.0 \mu\text{m}$ as the wavelength of an incident beam varies at $D_{\text{WGP}}/D_L = 1.0$. Whereas the NER and NTMT for $\Lambda = 0.5 \mu\text{m}$ are fairly constant with a deviation of less than 1%, those at $\Lambda = 1.0 \mu\text{m}$ vary strongly due to the Rayleigh anomaly effect. Note that the deviation is especially strong at shorter wavelengths. At longer wavelengths, the effect of the Rayleigh anomaly subsides so that the NER and NTMT converge to those of shorter wavelengths.

As mentioned earlier, a complete polarimeter, which measures an input scene at four different polarization angles to obtain full Stokes parameters, needs a WGP pixilated with wire grids in four different orientations. General results of the polarimetric performance uniformity for a single orientation re-

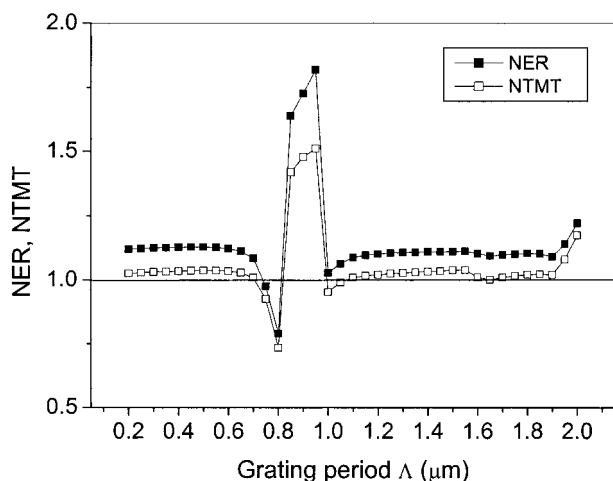


Fig. 4. NER and NTMT at $D_{\text{WGP}}/D_L = 1.0$ and $\lambda = 3 \mu\text{m}$ with the grating period. The f -number of an imaging lens is assumed to be fixed at 2. A reference line is also shown.

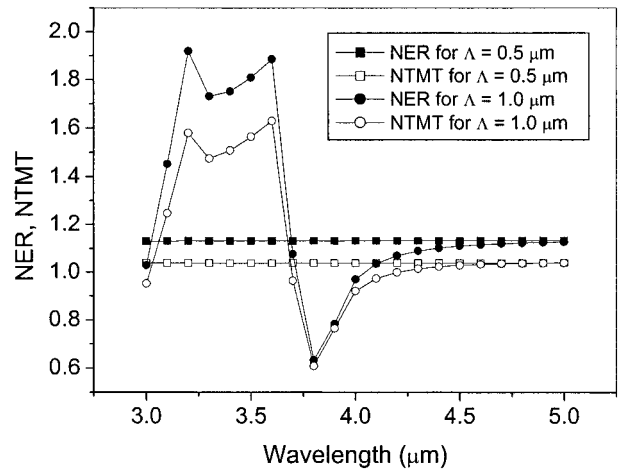


Fig. 5. NER and NTMT at $\Lambda = 0.5$ and $1.0 \mu\text{m}$ as the wavelength of an incident beam varies from 3 to $5 \mu\text{m}$. $D_{\text{WGP}}/D_L = 1.0$, and the f -number of an imaging lens is fixed at 2.

main equally valid for a WGP with multiple orientations. In this case, intrapixel nonuniformity among subpixels of different orientations within a WGP pixel exists in addition to pixel-to-pixel variation. The intrapixel deviation varies depending on the relative location of a WGP pixel and can be substantial if a pixel is large. However, the intrapixel deviation is much smaller than the pixel-to-pixel variation.

4. Discussion

The results obtained in the previous section suggest design considerations for an imaging polarimetry implementation that minimizes performance variation. First of all, based on the results presented in Fig. 2, it is beneficial to maintain an imaging aperture that is much wider than a WGP. This indicates that when an f -number of an imaging lens is fixed, a larger focal length benefits the uniformity, although it entails greater physical size. If the focal length is fixed, a lens of a larger f -number produces better optical uniformity. Such a lens is associated with an aperture narrower than that of a WGP and is subject to increased vignetting.¹⁷

Second, the results presented in Figs. 4 and 5 emphasize the presence of significant nonuniformity when a Rayleigh anomaly is excited and thus indicate that a WGP should be designed to circumvent the anomaly. In order not to excite higher-order diffraction, the grating period of wire grids should be smaller than that at which a Rayleigh anomaly occurs. Although a large grating period facilitates the fabrication process, Eqs. (3)–(5) indicate that the grating period of wire grids should suffice:

$$\Lambda < \frac{\lambda}{n_s \pm \sin \left[\tan^{-1} \frac{1}{2f/\#} \left(1 + \frac{D_{\text{WGP}}}{D_L} \right) \right]}, \quad (6)$$

where the + (–) sign in the denominator is associated

with the excitation of a first-order diffraction with $m = -1 (+1)$.

Note that the issue of the polarimetric performance uniformity is irrelevant to the sensor sensitivity. In other words, the performance nonuniformity due to the optical characteristics of a WGP is present in a polarimetric sensor system even with the best sensitivity of a sensor element, unless nonuniform sensitivity is intentionally introduced into a sensor to compensate for the effect of a WGP.

5. Conclusion

The variation of the polarimetric measures of a WGP, such as an ER and the TM transmittance, have been investigated with a simple numerical model based on rigorous coupled-wave analysis. The results show that the aperture ratio is a major parameter that can significantly affect the uniformity, whereas the effect of the grating thickness on the uniformity is relatively restricted. Even if the ratio is small, the design of a WGP should avoid incurring a Rayleigh anomaly since it causes a substantial increase in nonuniformity in the polarimetric performance, especially for an incident beam at short wavelengths. Minimizing the variation due to the characteristics of a WGP is important to reduce the likelihood of an error that an identical object is detected differently in imaging polarimetry.

This work was supported by the Korea Science and Engineering Foundation through the National Core Research Center for Nanomedical Technology (grant R15-2004-024-00000-0).

References

1. R. Tyan, A. Salvekar, H. Chou, C. Cheng, A. Scherer, F. Xu, P. C. Sun, and Y. Fainman, "Design, fabrication, and characterization of form-birefringent multilayer polarizing beam splitter," *J. Opt. Soc. Am. A* **14**, 1627–1636 (1997).
2. E. Chen and S. Y. Chou, "Polarimetry of thin metal transmission gratings in the resonance region and its impact on the response of metal-semiconductor-metal photodetectors," *Appl. Phys. Lett.* **70**, 2673–2675 (1997).
3. H. Tamada, T. Doumuki, T. Yamaguchi, and S. Matsumoto, "Al wire-grid polarizer using the *s*-polarization resonance effect at the 0.8- μm -wavelength band," *Opt. Lett.* **22**, 419–421, (1997).
4. M. H. Smith, J. D. Howe, J. B. Woodruff, M. A. Miller, G. R. Ax, T. E. Petty, and E. A. Sornsin, "Multispectral infrared Stokes imaging polarimeter," in *Polarization Measurement, Analysis, and Remote Sensing II*, D. H. Goldstein and D. B. Chenault, eds., Proc. SPIE **3754**, 137–143 (1999).
5. S. Arnold, E. Gardner, D. Hansen, and R. Perkins, "An improved polarizing beamsplitter LCOS projection display based on wire-grid polarizers," in *SID 01 Digest* (Society for Information Display, 2001), pp. 1282–1285.
6. X.-J. Yu and H.-S. Kwok, "Application of wire-grid polarizers to projection displays," *Appl. Opt.* **42**, 6335–6341 (2003).
7. D. Kim, "Polarization characteristics of a wire-grid polarizer in a rotating platform," *Appl. Opt.* **44**, 1366–1371 (2005).
8. C. H. Smith, T. J. T. Moore, D. K. Aitken, and T. Fujiyoshi, "NIMPOL: an imaging polarimeter for the mid-infrared," *Publ. Astron. Soc. Aust.* **14**, 179–188 (1997).
9. Y. Yao, N. Hirata, M. Ishii, T. Nagata, Y. Ogawa, S. Sato, and M. Watanabe, "Near-infrared polarimetric study of Monoceros R2 IRS," *Astrophys. J.* **490**, 281–290 (1997).
10. N. Ageorges and J. R. Walsh, "Acquisition and analysis of adaptive optics imaging polarimetry data," *Astron. Astrophys. Suppl. Ser.* **138**, 163–176 (1999).
11. G. P. Nordin, J. T. Meier, P. C. Deguzman, and M. W. Jones, "Micropolarizer array for infrared imaging polarimetry," *J. Opt. Soc. Am. A* **16**, 1168–1174 (1999).
12. M. Born and E. Wolf, *Principles of Optics* (Pergamon, 1980), Sec. 10.8.
13. F. A. Sadjadi and C. S. L. Chun, "Passive polarimetric IR target classification," *IEEE Trans. Aerosp. Electron. Syst.* **37**, 740–751 (2001).
14. D. Kim, C. Warde, K. Vaccaro and C. Woods, "Imaging multi-spectral polarimetric sensor: single-pixel design and fabrication," *Appl. Opt.* **42**, 3756–3764 (2003).
15. M. G. Moharam and T. K. Gaylord, "Rigorous coupled-wave analysis of metallic surface-relief gratings," *J. Opt. Soc. Am. A* **3**, 1780–1787 (1986).
16. E. D. Palik, *Handbook of Optical Constants of Solids*, (Academic, 1985).
17. W. J. Smith, *Modern Optical Engineering* (McGraw-Hill, 1990) pp. 135–139.